LBL-35821
UC-413
Preprint

Lawrence Berkeley Laboratory
UNIVERSITY OF CALIFORNIA

Submitted to Physical Review Letters

Consequences of Nuclear Shadowing for Heavy Quarkonium Production in Hadron-Nucleus Interactions

S. Liuti and R. Vogt

July 1994

REFERENCE COPY
Does Not
Circulate
Bldg. 50 Library.
LBL-35821
Copy 1

Prepared for the U.S. Department of Energy under Contract Number DE-AC03-76SF00098

DISCLAIMER

This document was prepared as an account of work sponsored by the United States Government. While this document is believed to contain correct information, neither the United States Government nor any agency thereof, nor the Regents of the University of California, nor any of their employees, makes any warranty, express or implied, or assumes any legal responsibility for the accuracy, completeness, or usefulness of any information, apparatus, product, or process disclosed, or represents that its use would not infringe privately owned rights. Reference herein to any specific commercial product, process, or service by its trade name, trademark, manufacturer, or otherwise, does not necessarily constitute or imply its endorsement, recommendation, or favoring by the United States Government or any agency thereof, or the Regents of the University of California. The views and opinions of authors expressed herein do not necessarily state or reflect those of the United States Government or any agency thereof or the Regents of the University of California.

LBL-35821
July 1994

Consequences of Nuclear Shadowing for Heavy Quarkonium Production in Hadron-Nucleus Interactions*

S. Liuti

Nuclear Science Division, Lawrence Berkeley Laboratory, Berkeley CA 94720, USA

and

I.N.F.N. Sezione Sanitá

Viale Regina Elena 299, I-00161 Rome, Italy

R. Vogt

Nuclear Science Division, Lawrence Berkeley Laboratory, Berkeley CA 94720, USA

Abstract

We study nuclear shadowing in J/ψ and Υ production in hadron-nucleus interactions and in nucleus-nucleus collisions at the Relativistic Heavy Ion Collider and the Large Hadron Collider. As a consequence of the perturbative Q^2-dependence of gluon shadowing, we predict that Υ production is less suppressed than the J/ψ. We show that antishadowing leads to enhanced J/ψ production at $x_f \lesssim 0$, an effect reduced for Υ production.

* This work was supported in part by the Director, Office of Energy Research, Division of Nuclear Physics of the Office of High Energy and Nuclear Physics of the U. S. Department of Energy under Contract Number DE-AC03-76SF0098.

The production of charmonium and bottomonium states in hadron-nucleus interactions does not increase linearly with the nuclear target size A. Additionally, the ratio of hadron-nucleus to hadron-nucleon production, $S_A = \sigma_{hA}/A\sigma_{hp}$, is not constant but decreases as a function of the fraction of the center of mass momentum, x_f, carried by the produced resonance. There are several effects that contribute both to the A dependence of the total cross section and to the ratio S_A including nuclear absorption [1], comover interactions [2], intrinsic heavy quark states [3], projectile energy loss [4], and nuclear shadowing [5,6].

In this paper, we examine the role of shadowing of the nuclear parton distributions in quarkonium production. Nuclear shadowing modifies the target parton distributions so that $xq^A(x) \neq Axq^N(x)$. Deep inelastic scattering (DIS) data on the ratio $R_A = F_2^A/F_2^D$ [7,8] show that: *i)* nuclear shadowing begins to set in at $x_{Bj} \lesssim 0.06$ for all nuclei ($R_A < 1$); *ii)* R_A has a very weak Q^2 dependence; and *iii)* an enhancement, or *antishadowing*, exists for $0.06 \lesssim x_{Bj} \lesssim 0.25$ ($R_A > 1$). In addition, the NMC data on J/ψ production with Sn and C targets show an enhancement of $(13 \pm 8)\%$ for $0.05 \lesssim x_{Bj} \lesssim 0.3$ [9], interpreted as gluon antishadowing.

The weak Q^2 dependence of R_A is consistent with the models of [10,11], where nuclear shadowing is considered as a leading-order QCD effect with perturbatively generated Q^2 dependence. These models differ in the treatment of the nonperturbative contribution at the initial scale Q_0^2. We adopt the QCD Aligned-Jet Model (QAJM) [11] which accounts for the DIS data [11,12] to study the effect of nuclear shadowing on S_A.

We would like to point out two major consequences of shadowing and antishadowing for J/ψ and Υ hadroproduction based on very general arguments. Since m_Υ is three times larger than m_ψ, the Υ is primarily produced within the antishadowing region of the target at present energies. However, the parton distributions are evaluated at $Q^2 = m_\Upsilon^2$, thus Q^2 evolution reduces the effect of both shadowing and antishadowing in Υ production with respect to J/ψ. The antishadowing apparently present in both the DIS measurements of R_A [7,8] and the gluon distribution [9] reflects on S_A. We include the observed antishadowing effect, a general consequence of baryon number and momentum conservation in a nucleus,

and explore the consequences of Q^2 evolution on S_A.

We do not expect our shadowing model to fully explain the shape and magnitude of S_A. To quantitatively show the effects of nuclear shadowing, we have not included other A dependent effects. Nuclear absorption and comover interactions do not have a strong x_f dependence and mainly affect the magnitude of S_A [1,2]. On the other hand, intrinsic heavy quarks [3] and projectile energy loss [4] have a significant x_f dependence.

The leading order $Q\overline{Q}$ bound state cross section is the integral of the free $Q\overline{Q}$ production cross section from the $Q\overline{Q}$ threshold to the meson pair threshold,

$$\frac{d\sigma}{dx_f} = 2F \int_{2m_Q/\sqrt{s}}^{2m_H/\sqrt{s}} \tau d\tau \frac{H_{pt}(x_1, x_2; x_1 x_2 s)}{\sqrt{x_f^2 + 4\tau^2}} , \tag{1}$$

where $m_c = 1.5$ GeV, $m_b = 4.75$ GeV, $m_D = 1.867$ GeV, and $m_B = 5.28$ GeV. The bound state fraction, F, is a parameter that cancels in S_A. We include quark–antiquark annihilation and gluon–gluon fusion subprocesses in the convolution formula H_{pt},

$$\begin{aligned} H_{pt}(x_1, x_2; m^2) &= G_p(x_1) G_t(x_2) \sigma(gg \to Q\overline{Q}; m^2) \\ &+ \sum_{q=u,d,s} (q_p(x_1)\overline{q}_t(x_2) + \overline{q}_p(x_1) q_t(x_2)) \sigma(q\overline{q} \to Q\overline{Q}; m^2) , \end{aligned} \tag{2}$$

where $x_{1,2} = \frac{1}{2}(\pm x_f + \sqrt{x_f^2 + 4\tau^2})$ are the projectile and target momentum fractions. We use the MRS D$-'$ [13] distributions that describe the recent HERA data on F_2^{ep} [14].

Next-to-leading order contributions to the free $Q\overline{Q}$ cross section have been calculated. The x_f distribution is approximately that from lowest order multiplied by a theoretical K factor, $\sigma(\alpha_s^3)/\sigma(\alpha_s^2)$ [15], assumed to be absorbed in F. At lowest order, the J/ψ is produced with $p_T = 0$ since the $c\overline{c}$ pair is back-to-back. A p_T dependence may be introduced through an intrinsic transverse momenta, q_T, of the initial partons as we show later. For $p_T \gg m_{\rm res}$, higher-order corrections are needed [16]. Since we concentrate on the x_f distributions and the A dependence, where $p_T \lesssim m_{\rm res}$ is dominant, our calculation is lowest order.

When the target is a nucleus, the parton distributions, $G_t(x_2)$, $q_t(x_2)$ and $\bar{q}_t(x_2)$ in Eq. (2) are the nuclear medium modified distributions evaluated at $Q^2 \approx m_\psi^2$ and $Q^2 \approx m_\Upsilon^2$ for J/ψ and Υ production. We calculate the shadowed distributions at the initial scale, $Q^2 =$

$Q_0^2 \approx 5\,\mathrm{GeV}^2$, and $x < x_{sh} \approx 0.04$ according to the QAJM [11] and evolve in Q^2 using the Dokshitser-Gribov-Lipatov-Altarelli-Parisi equations (DGLAP) [17]. Recombination effects within a single nucleon are negligible at $x \gtrsim 10^{-3}$ [5,18]. In the QAJM, shadowing is generated by the interaction of hadronic configurations originating from fluctuations of the virtual photon with small transverse momentum, or jets *aligned* along the direction of the virtual photon, $\vec{\mathbf{q}}/|\mathbf{q}|$, with $k_\perp < k_{0\perp} \approx 0.4\,\mathrm{GeV}$. The transverse separation of the aligned jets is correspondingly large (≈ 1 fm) and their phase space is restricted by a factor $\propto k_{0\perp}^2/M^2$. In QCD the transverse momentum of the fluctuation can be large so that *nonaligned* hadronic configurations are simultaneously present. Such configurations interact differently in the nuclear medium. In Refs. [11,12] it was assumed that aligned jets with large transverse separation interact in the nucleus as vector mesons. Nonaligned jets, with $k_\perp > k_{0\perp}$ and a small transverse separation have a correspondingly small interaction cross section, giving rise to color transparency.

The nuclear baryon number and momentum sum rules:

$$\frac{1}{A}\int_0^A dx V_A(x,Q^2) = \int_0^1 dx V_N(x,Q^2)\ , \tag{3a}$$

$$\frac{1}{A}\int_0^A dx x[V_A(x,Q^2) + G_A(x,Q^2) + S_A(x,Q^2)] = \int_0^1 dx x[V_N(x,Q^2) + G_N(x,Q^2) + S_N(x,Q^2)]\ , \tag{3b}$$

must be fulfilled at every Q^2. In Eq. (3b) $V_{N(A)} \equiv u_t^V + d_t^V$, $S_{N(A)} \equiv 2(\overline{u}_t + \overline{d}_t + \overline{s}_t)$, and $G_{N(A)} \equiv G_t$, are the nucleon, N, and nuclear, A, valence, sea and gluon distributions. In order to satisfy the sum rules and simultaneously allow for shadowing at $x \lesssim 0.04$, the parton distributions must be enhanced at higher values of x. We assume that the enhancement is shared by the valence quarks and gluons since the sea quark enhancement is consistent with zero [19] (see also Ref. [12]). Recent data from E665 [8] show that the enhancement in R_A is concentrated in the interval $0.06 \lesssim x \lesssim 0.25$ and is A-independent. These two crossover points, assuming no sea enhancement, are sufficient to constrain the valence and gluon antishadowing.

Gluon shadowing should be larger than sea quark shadowing since the interaction of

a $q\bar{q}g$ configuration in the γ^* wavefunction with the target should be stronger than a $q\bar{q}$ configuration [20,21]. Indeed, the perturbative interaction cross section of a small color octet with a nucleon is 9/4 larger than a color triplet of the same transverse size. Assuming a smooth connection between the perturbative and nonperturbative domains, $\sigma_{\gamma^*\to q\bar{q}g,N} = \frac{9}{4}\sigma_{\gamma^*\to q\bar{q},N}$, leading to larger effects on the gluon relative to the sea and valence quarks [20]. The overall enhancement found in [12,20] is consistent with the data of [9], used to constrain the shape of the gluon distribution in the antishadowing region. A weak Q^2 dependence for R_A is obtained, in accord with the data of [7,8], while a stronger Q^2 dependence is found for the gluon ratio, $R_A^G = G_A/G_N$. Similar results were also obtained in [22].

In Fig. 1 we show x_2 as a function of x_f for J/ψ (solid curve), Υ (dashed) production for several energies to point out the shadowing and antishadowing regions. At 200 GeV, 1(a), the J/ψ is antishadowed for $0 \lesssim x_f \lesssim 0.6$. At 800 GeV, 1(b), where data exists for J/ψ and Υ from $-0.2 < x_f < 0.65$ [23], the J/ψ lies in the shadowing region for $x_f > 0$ but enters the antishadowing region at backward values. The Υ is mainly produced in the antishadowing region, but when $x_f < 0$, it is in the EMC region. Since the parton distributions are evaluated at m_Υ^2 and the gluon distribution evolves faster than the quarks, we expect $S_A^\Upsilon > S_A^\psi$ for $x_f > 0$. In 1(c) and 1(d), the x_f range corresponds to $-0.35 < y < 2.5$ and $|y| < 1$, the rapidity coverage of the PHENIX [24] and ALICE [25] detectors at RHIC ($\sqrt{s} = 200A$ GeV) and the LHC ($\sqrt{s} = 5.5$ TeV), respectively. At RHIC central rapidities the Υ may still be antishadowed, but would be detected in the shadowing region with the muon spectrometer [24]. At the LHC, both J/ψ and Υ production are shadowed.

The shadowing and antishadowing features of S_A are shown explicitly in Fig. 2 where we compare S_A^ψ and S_A^Υ to the E772 data at 800 GeV on C, Ca, Fe, and W targets [23]. Recall that when x_f is increasing, x_2 is decreasing. The solid curves show S_A^ψ, the dashed, $S_A^{\psi'}$, and the short dashed, S_A^Υ. The difference between J/ψ and ψ' comes from their small mass difference. Antishadowing is clearly seen for the J/ψ as $x_f \to 0$. Antishadowing at negative x_f is in contradiction with the data: clearly other effects are needed to account for this behavior. The effect of Q^2 evolution on S_A^Υ is apparent–the antishadowing peak is

broader and closer to unity than the corresponding region of S_A^ψ. The Υ enters the EMC region for $x_f < 0$, decreasing S_A^Υ. While this trend agrees with the shape of the data, the magnitude is too large.

Accounting for the primordial transverse momentum of the partons, q_T, may reduce the magnitude of S_A since the transverse momentum spectrum may be broadened in a nucleus because of Fermi motion. If the cross sections are integrated over all p_T, the q_T smearing will have no effect (the q_T spectrum in a moving nucleon has the same normalization as for a stationary one). However, the data is taken over a finite range of p_T, suggesting that the broader q_T smearing in the nucleus manifests itself in a reduced p_T-integrated cross section relative to the nucleon, reducing S_A. We calculated the q_T spectra in nuclei by smearing the primordial transverse momentum distribution in a free nucleon with nucleon momentum distributions from realistic many-body calculations [26]. The primordial q_T spectrum for a free nucleon was parametrized by a gaussian with $\langle q_T^2 \rangle \approx 1\text{GeV}^2$, the same form used to describe the low p_T Drell-Yan data in pp scattering [28]. Similar values of $\langle q_T^2 \rangle$ are also compatible with the low p_T data for J/ψ production [29]. The convolution formula also involves longitudinal degrees of freedom and is therefore x dependent, producing an x_f-dependent effect on S_A. A detailed description of our calculation will be shown in a more extended paper [27]. The nuclear q_T smearing shown in Fig. 2(b) and in Fig. 2(d) for the J/ψ (dotted curves) and in Fig. 2(d) for Υ (dot-dashed curve), reduces the effect of antishadowing and affects the shadowing part only marginally because of its increasing behavior with x (decreasing with x_f). The agreement with data is substantially improved.

In Fig. 3(a) we compare the model with the E772 Drell-Yan production data [19] in the W target as a check on the role of sea quark shadowing and the effect of Q^2 evolution. The model, including a small effect from q_T smearing (dotted curve), indeed gives a good description of the data. We show a comparison with the NA3 J/ψ production data from 200 GeV proton interactions with ^{2}H and Pt targets [29] in 3(b). The antishadowing region is broad with shadowing only for $x_f > 0.4$. The width of the antishadowing peak decreases

with increasing energy since x_2 passes from the shadowing region to the EMC regime over a smaller range of x_f. The antishadowing region is also shifted backward with x_f as the energy grows, indicated by a comparison of S_A^ψ in Fig. 2(d) and Fig. 3(b). Clearly nuclear shadowing alone, and even including the p_T-integrated spectra, does not account for the observed suppression. Other effects become important and must be taken into account [3].

Finally, we predict the shadowing of J/ψ, Υ, and Drell-Yan production in Au+Au collisions at RHIC energy relative to pp production at the same energy in Fig. 3(c). Both the projectile and target distributions are shadowed. RHIC data will not be strongly affected by antishadowing, as expected from Fig. 1(c). Since only relatively small x_f values can be measured, features important at large x_f will not play a role. Thus shadowing will dominate the nuclear effects. We expect this behavior to be even more pronounced for LHC, where the range in x extends below $x = 10^{-3}$, Fig. 1(d). Here recombination effects should play an important role and could be tested accurately. Calculations including recombination effects at LHC energies are in progress and will be shown elsewhere [27].

We have evaluated the effect of shadowing on heavy quarkonium production in current experiments and at RHIC. Because of their difference in mass, J/ψ and Υ production follow different patterns. Antishadowing has been shown to be substantial at present energies, in particular, Υ production is within the antishadowing region. However the amount of shadowing and antishadowing for Υ is smaller than for the J/ψ because of the perturbative Q^2 evolution of the shadowed distributions. Nuclear modifications of the primordial transverse momentum spectrum are an important addition in the low p_T range.

Nuclear shadowing is an important feature of quarkonium production, yet at lower energies it is not sufficient. Shadowing will play a major role in nucleus-nucleus collisions, suppressing both J/ψ and Υ production significantly but according to different patterns in x_f, over an extrapolation from pp interactions.

We thank K. J. Eskola, L. Frankfurt, S. Gavin, I. Hinchcliffe, B. Kopeliovich, K.B. Luk, J. Peng, H. Schellman, M. Strikman and X.-N. Wang for useful discussions. S.L. would like to thank the Nuclear Theory Group at the Lawrence Berkeley Laboratory for their warm

hospitality.

REFERENCES

[1] C. Gerschel and J. Hüfner, Phys. Lett. **B207** (1988) 254.

[2] S. Gavin and R. Vogt, Nucl. Phys. **B345** (1990) 104. S. Gavin, H. Satz, R.L. Thews, and R. Vogt, Z. Phys. **C61** (1994) 351.

[3] R. Vogt, S.J. Brodsky, and P. Hoyer, Nucl. Phys. **B360** (1991) 67.

[4] S. Gavin and J. Milana, Phys. Rev. Lett. **68** (1992) 1834; S.J. Brodsky and P. Hoyer, Phys. Lett. **B298** (1993) 165; D. Kharzeev and H. Satz, Z. Phys. **C60**, (1993) 389.

[5] A.H. Mueller and J. Qiu, Nucl.Phys. **B268**, 427 (1986); J. Qiu, Nucl. Phys. **B291**, (1988) 746.

[6] S. Gupta and H. Satz, Z. Phys. **C55** (1992) 391.

[7] M. Arneodo, CERN-PPE/92-113, to be published in Phys. Rep.

[8] T. Carroll, Thesis 1993; T. Carroll *et al.*, FNAL Conf-93/166-E and *Proceedings of the XXVII Rencontres de Moriond*, March 21-27, 1993.

[9] M. Arneodo *et al.* (NMC Collaboration), Nucl. Phys. **371** (1992) 553.

[10] N.N. Nikolaev and B.G. Zakharov, Phys. Lett. **B260** (1991) 414. S.J. Brodsky and H.J. Lu, Phys. Rev. Lett. **64** (1990) 1342.

[11] L. Frankfurt and M. Strikman, Phys. Rep. **160**, 235 (1988); Nucl. Phys. **B316**, 340 (1989).

[12] L. Frankfurt, M. Strikman, and S. Liuti, Phys. Rev. Lett. **65** (1990) 1725.

[13] A.D. Martin, W.J. Stirling, and R.G. Roberts, Phys. Lett. **B306**, 145 (1993)

[14] ZEUS Collaboration, M. Derrick *et al.*, DESY preprint 93-110, Phys. Lett. (to be published).

[15] M.L. Mangano, P. Nason, and G. Ridolfi, Nucl. Phys. **B373** (1992) 295; Nucl. Phys. **B405** (1993) 507.

[16] R.K. Ellis and J.C. Sexton, Nucl. Phys. **B269** (1986) 445.

[17] V.N. Gribov and L.N. Lipatov, Sov. J. Nucl. Phys. **15** (1972) 438; L.N. Lipatov, Sov. J. Nucl. Phys. **20** (1974) 181; Yu.L. Dokshister, Sov.Phys. JETP **46** (1977) 641; G. Altarelli and G. Parisi, Nucl. Phys. **B216** (1977) 298.

[18] K.J. Eskola, J. Qiu and X. Wang, Phys. Rev. Lett **72**, 36 (1994).

[19] D.M. Alde *et al.*, Phys. Rev. Lett. **64** (1990) 2479.

[20] S. Liuti, L. Frankfurt, M. Strikman, and A. Yoshida, *Proceedings of the XXIX Rencontres de Moriond*, March 21-27, 1994, Ed. J. Tran Than Van.

[21] N.N. Nikolaev and B.G. Zakharov, Preprint KFA-IKP(Th)-1993-17, Landau-16/93, submitted to Z. für Phys. **C**.

[22] K.J. Eskola, Nucl. Phys. **B400** (1993) 240.

[23] D.M. Alde *et al.*, Phys. Rev. Lett. **66** (1990) 133.

[24] PHENIX Conceptual Design Report, 1993 (unpublished).

[25] ALICE Letter of Intent, CERN Report No. CERN/LHCC/93-16, 1993 (unpublished).

[26] O. Benhar *et al.*, Phys. Lett. **177B** (1986) 135.

[27] S. Liuti and R. Vogt, in preparation.

[28] D. Antreasyan *et al.*, Phys. Rev. Lett. **48** (1982) 302.

[29] J. Badier *et al.*, Z. Phys. **C20** (1983) 101.

Figure Captions

Figure 1. A comparison of x_2 as a function of x_f for J/ψ (solid) and Υ (dashed) production, at (a) 200 GeV and (b) 800 GeV fixed target energies and (c) RHIC and (d) LHC ion collider energies.

Figure 2. Our model calculations for S_A^{ψ} (solid), $S_A^{\psi'}$ (dashed), and S_A^{Υ} (dotted) compared to data from (a) C, (b) Ca, (c) Fe, and (d) W targets at 800 GeV [19]. The Υ data is shown on (d) only. The effect of q_T broadening in the nucleus is shown in (b) and (d) for S_A^{ψ} (dotted) and in (d) for Υ (dot-dashed).

Figure 3. (a) A calculation of S_A^{DY} with the data from Ref. [23] at 800 GeV on the W target (solid). The dotted curve shows the effect of q_T broadening. (b) The J/ψ production data of Ref. [29] on ^{2}H and Pt targets at 200 GeV compared with S_A^{ψ}. (c) Predictions of S_{AA}^{ψ} (solid), $S_{AA}^{\psi'}$ (dashed), S_{AA}^{Υ} (short-dashed), and S_{AA}^{DY} (dotted) for Au+Au collisions at RHIC.

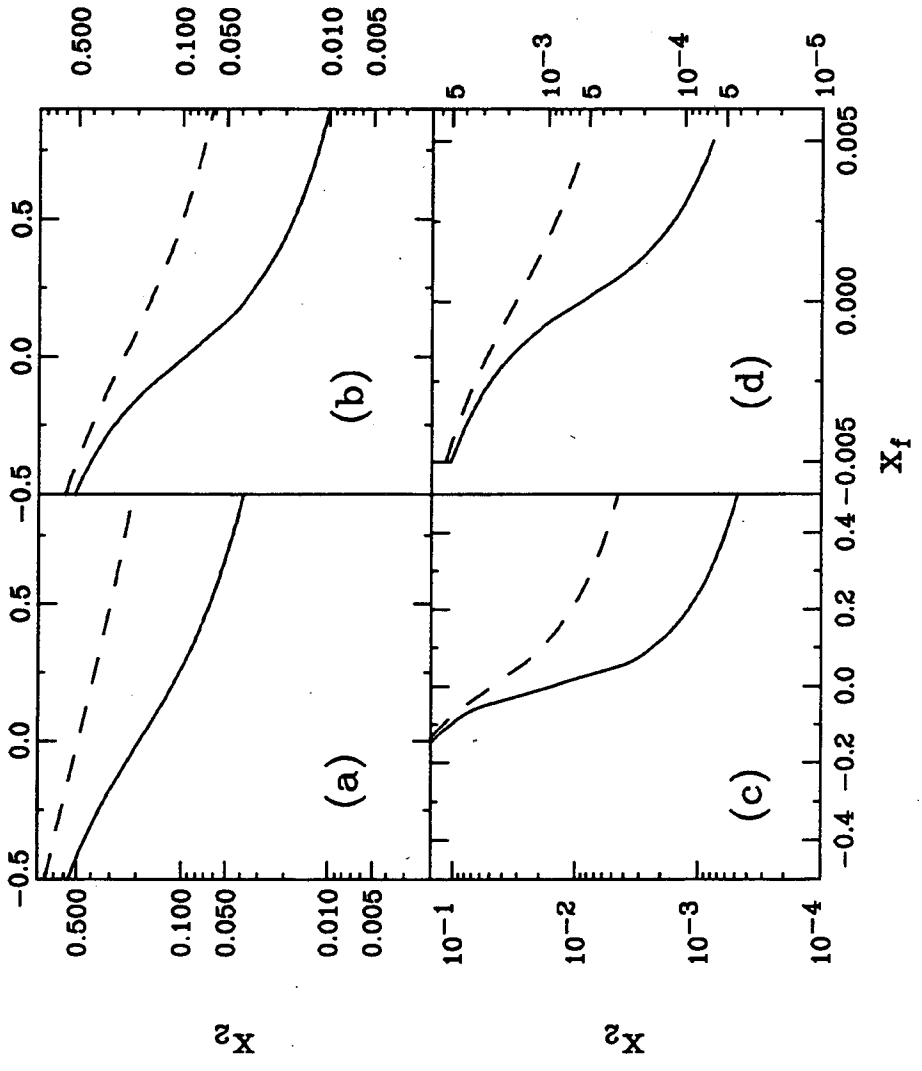
(a)
(b)
(c)
(d)
x_2
x_2
x_f
0.500
0.100
0.050
0.010
0.005
10^{-1}
10^{-2}
10^{-3}
10^{-4}
10^{-5}
5
−0.5
0.0
0.5
−0.4
−0.2
0.2
0.4
−0.005
0.000
0.005

Figure 1

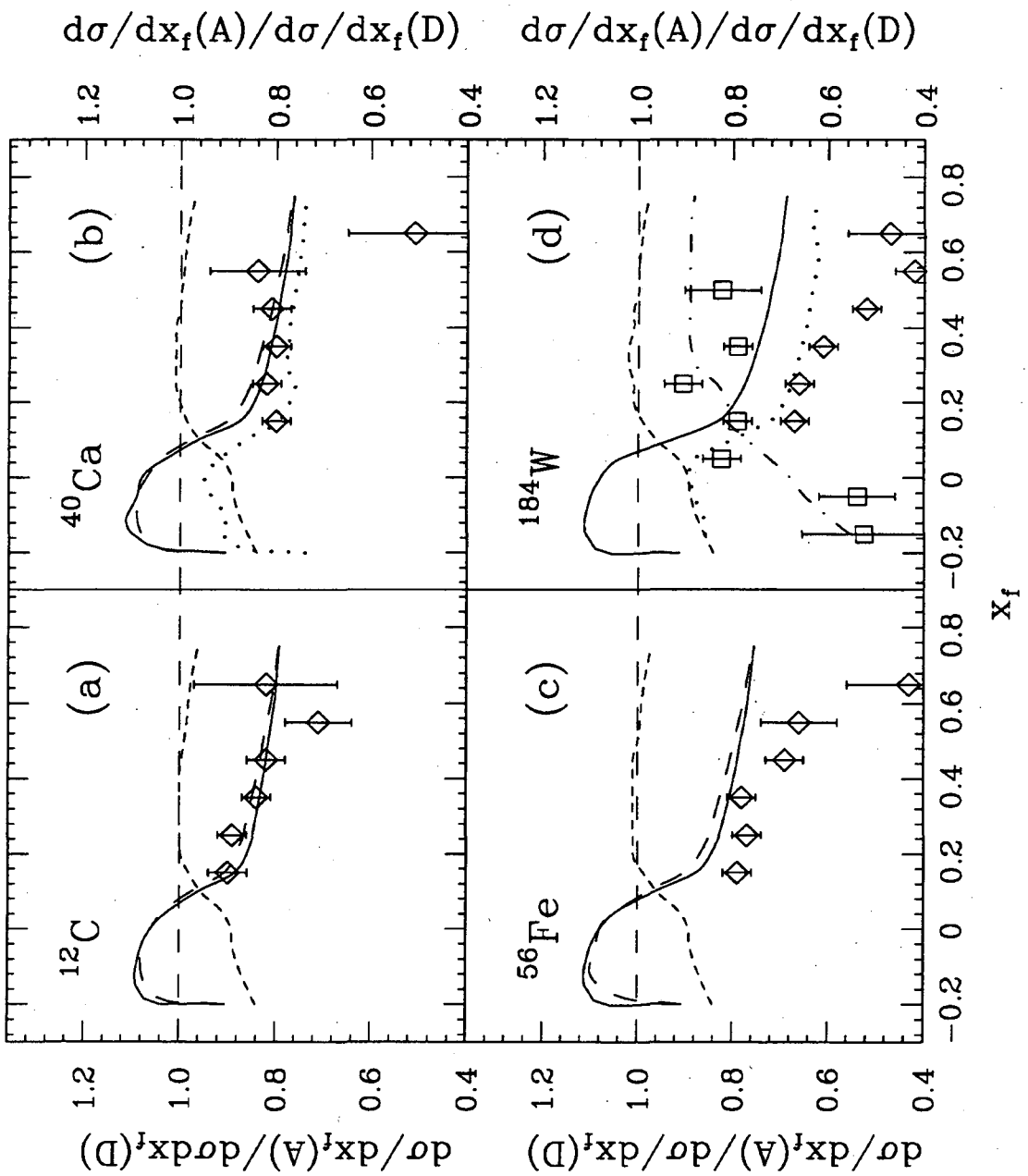
dσ/dx_f(A)/dσ/dx_f(D)
dσ/dx_f(A)/dσ/dx_f(D)
(a)
(b)
(c)
(d)
12C
40Ca
56Fe
184W
dσ/dx_f(A)/dσdx_f(D)
dσ/dx_f(A)/dσ/dx_f(D)
x_f

Figure 2

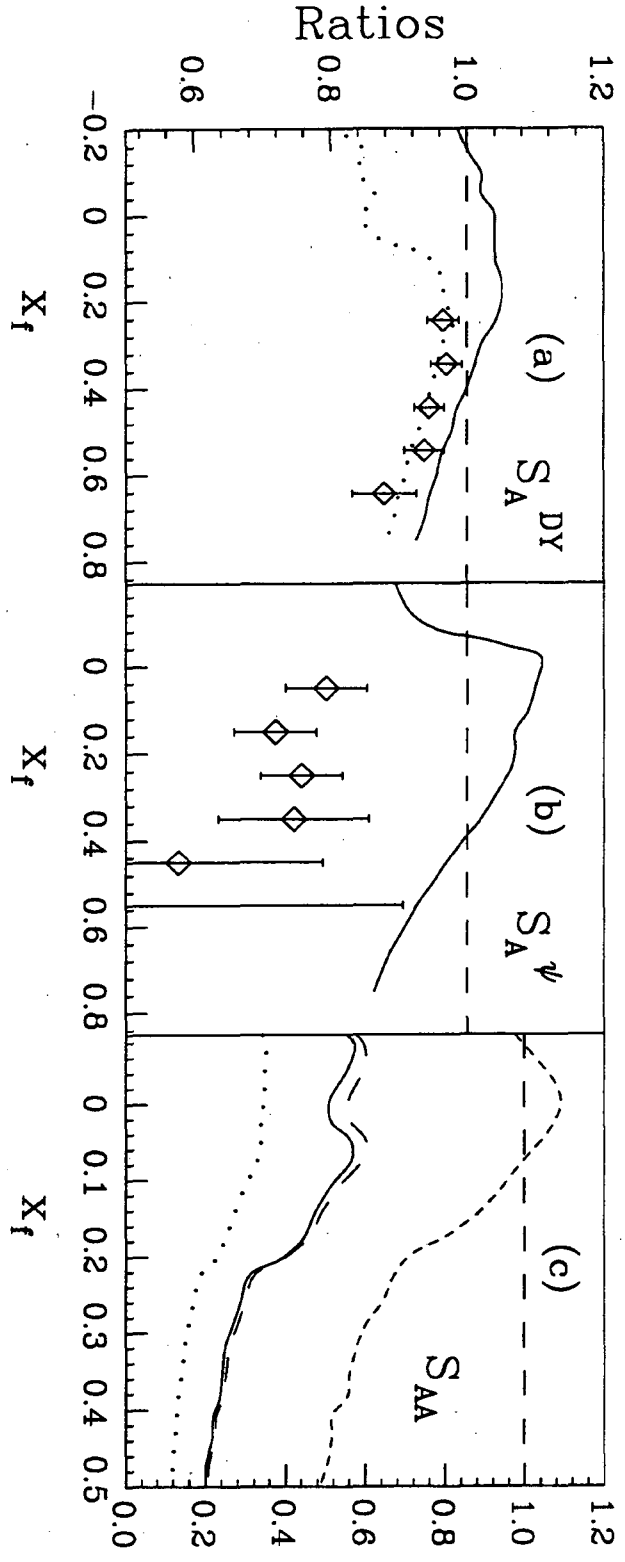

Figure 3

LAWRENCE BERKELEY LABORATORY
UNIVERSITY OF CALIFORNIA
TECHNICAL INFORMATION DEPARTMENT
BERKELEY, CALIFORNIA 94720